Thermal Induced Modulation of Surface Charge of Sialoglycosphingolipid Micelles

ARTICLE *in* THE JOURNAL OF PHYSICAL CHEMISTRY B · NOVEMBER 1999

Impact Factor: 3.3 · DOI: 10.1021/jp991330c

3 AUTHORS, INCLUDING:

Mitsuhiro Hirai
Gunma University
98 PUBLICATIONS **1,183** CITATIONS
SEE PROFILE

Hiroki Iwase
CROSS-Tokai
48 PUBLICATIONS **578** CITATIONS
SEE PROFILE

Thermal Induced Modulation of Surface Charge of Sialoglycosphingolipid Micelles

Mitsuhiro Hirai,* Hiroki Iwase, and Tomohiro Hayakawa

Department of Physics, Gunma University, Maebashi 371-8510, Japan

Received: April 22, 1999; In Final Form: July 19, 1999

In the present study, by using a shell-modeling method under a rescaled mean spherical approximation (RMSA) for charged particle dispersions, we have found that the thermal structural change of sialoglycosphingolipid micelles accompanies a change of the micellar surface charge, which greatly depends on the oligosaccharide chains. Here, we treat three different types of glycosphingolipids (monosialoganglioside, disialoganglioside, and trisialoganglioside). This phenomenon is induced by a variation of temperature in the physiological temperature range 20−40 °C, which is in agreement with our recent reports showing that the thermal induced shrinkage of the hydrophilic portion of the ganglioside micelles accompanies extrusion of water. The present and previous results strongly suggest that ganglioside molecules localized in outer cell membranes are able to modulate locally both electrostatic charge potential and hydrophilicity of cell surfaces through ganglioside-rich microdomains. These functional properties of gangliosides would play an important role in regulation of various physiological cell surface events such as an adhesion between cells or protein binding to the cell surface.

Introduction

Gangliosides, which are usually relatively minor components of vertebrate plasma membranes, appear to be the most abundant sialoglycosphingolipids in nerve cells.[1] Physiological functions of gangliosides have been clarified by many investigators to participate in various cell surface events such as self-organization of tissues, immune response, and cell differentiation through molecular recognition depending on the varieties of ganglioside structures.[2−5] Ganglioside is composed of a ceramide as a hydrophobic tail and of an oligosaccharide chain containing one or more *N*-acetylneuraminic acid (sialic acid) residues as a hydrophilic head. It is important for understanding physiological functions of gangliosides to elucidate physicochemical characteristics of gangliosides. Many studies of gangliosides and mixtures with other lipids have been done by using various methods such as NMR, calorimetry, scattering methods, and other techniques.[6−10] Despite those studies, the stability of ganglioside aggregate structures under various conditions is still ambiguous in comparison with the intensive knowledge of phospholipid systems whose phase behavior and physicochemical characteristics have been clarified precisely.

By using neutron and X-ray scattering techniques and calorimetry, we have been studying the structural phase behavior of ganglioside aggregates depending on temperature,[11−16] pH, and concentration.[17] We have also clarified the binding specificity of gangliosides with proteins depending on both oligosaccharide chain and protein surface modification.[18−20] We have shown the following results on the thermal structural stability of ganglioside micelles. The hydrophilic portions of ganglioside molecules composed of oligosaccharide chains sensitively change the conformations depending on temperature,[11−14] which accompanies intensive occlusion and extrusion of water in the hydrophilic portion of ganglioside micelle.[15,16] In another report[17] we presented the simultaneous determination procedure of the internal and external structures of the ganglioside micelles by using a shell-modeling method combined with a rescaled mean spherical approximation of interparticle interaction. In the present report, by analyzing interparticle interactions of three different types of ganglioside micelles, we will clarify another remarkable feature of ganglioside micellar charge, which greatly depends on both temperature and oligosaccharide chain.

Experimental Section

Sample Preparation. Gangliosides from bovine brain purchased from Sigma Chemical Co., Ltd. were used without further purification. Three different types of gangliosides used were $IV^3NeuAc\alpha$-$II^3NeuAc\alpha_2$-$GgOse_4Cer$ abbreviated as G_{T1b}, $IV^3NeuAc\alpha$-$II^3NeuAc\alpha$-$GgOse_4Cer$ abbreviated as G_{D1a}, and $II^3NeuAc\alpha$-$GgOse_4Cer$ abbreviated as G_{M1}. The full structures of the oligosaccharide portions of the G_{M1}, G_{D1a}, and G_{T1b} gangliosides are presented in Table 1. The samples used for the scattering experiments were prepared by dissolving the ganglioside lyophilized powder of 5% w/v in pure water purified by using Barnstead NANO Pure II. The low-concentration solutions, 0.5% w/v ganglioside solutions, were also used as control samples.

Small-Angle X-ray Scattering Measurements. Small-angle X-ray scattering experiments were performed by using the synchrotron radiation small-angle X-ray scattering spectrometer installed at the BL10C line of the 2.5 GeV storage ring at the Photon Factory at the National Laboratory for High Energy Physics, Tsukuba, Japan.[21] The wavelength used was 1.49 Å, and the sample-to-detector distance was 60 cm. The sample was contained in a sample cell with a pair of mica windows. The sample cell was placed in a cell holder whose temperature was varied from 10 to 70 °C. The exposure time for one measurement was 4 min.

Scattering Data and Modeling Analysis Methods. To estimate a radius of gyration R_g, we used Glatter's method as follows.[22]

* To whom correspondence should be addressed. Telefax: INT+81 272-20-7551 or 7552. Phone: INT+81 272-20-7554. E-mail: hirai@sun.aramaki.gunma-u.ac.jp.

10.1021/jp991330c CCC: $18.00
Published on Web 11/03/1999

TABLE 1: Structures of Gangliosides Used in This Paper

glycolipid	structure[a]
G_{M1}	Galβ1-3GalNAcβ1-4(NeuAcα2-3)Galβ1-4Glcβ1-1Cer
G_{D1a}	NeuAcα2-3Galβ1-3GalNAcβ1-4(NeuAcα2-3)Galβ1-4Glcβ1-1Cer
G_{T1b}	NeuAcα2-3Galβ1-3GalNAcβ1-4(NeuAcα2-8NeuAcα2-3)Galβ1-4Glcβ1-1Cer

[a] Structures are represented according to the recommendations introduced by the IUPAC-IUB Commission on Biochemical Nomenclature.

$$R_g^2 = \frac{\int_0^{D_{max}} p(r)\, r^2\, dr}{2\int_0^{D_{max}} p(r)\, dr} \quad (1)$$

where $p(r)$ is the distance distribution function. The $p(r)$ function was calculated by the Fourier inversion of the scattering curve $I(q)$ as

$$p(r) = \frac{2}{\pi}\int_0^{\infty} rq\, I(q)\, \sin(rq)\, dq \quad (2)$$

where q is the magnitude of scattering vector defined by $q = (4\pi/\lambda)\sin(\theta/2)$ (q, the scattering angle; λ, the wavelength), D_{max} is the maximum dimension of the particle estimated from the $p(r)$ function satisfying the condition $p(r) = 0$ for $r > D_{max}$. By using both the shell-modeling method and the rescaled mean spherical approximation, we can determine the intraparticle structure and the interparticle interaction separately.[17] For a monodispersion composed of identical particles interacting with each other, the scattering function is generally given by

$$I(q) \propto N\, I_s(q)\, S(q) \quad (3)$$

where N is the number concentration of the particles, $I_s(q)$ the scattering function of the particle, and $S(q)$ the interparticle structure factor obtained by Fourier transforming the interparticle correlation function. As we have shown elsewhere,[11−17,23,24] the spherically averaged scattering function $I_s(q)$ from a particle described by n shells with different average scattering densities is simply given by

$$I_s(q) = \int_0^1 \left\{ 3\left[\frac{\bar{\rho}_1 V_1 j_1(qR_1)}{qR_1} + \sum_{i=2}^{n} \frac{(\bar{\rho}_i - \bar{\rho}_{i-1}) V_i j_1(qR_i)}{qR_i} \right] \right\}^2 dx \quad (4)$$

where $\bar{\rho}_i$ is the average excess scattering density (so-called contrast) of ith shell with a shape with an ellipsoid of rotation and j_1 is the spherical Bessel function of the first rank. R_i is defined as

$$R_i = r_i(1 + x^2(\upsilon_i^2 - 1))^{1/2} \quad (5)$$

where r_i and υ_i are the semiaxis and semiaxial ratio of ith ellipsoidal shell, respectively. $\bar{\rho}_i$, r_i, and υ_i were used as fitting parameters. In the scheme of the rescaled mean spherical approximation the interparticle structure factor $S(q)$ for identical macroions interacting through a repulsive screened Coulomb potential is given as

$$S(q) = \frac{1}{1 - 24\eta\, a(q\sigma)} \quad (6)$$

where $\eta = \pi N\sigma^3/6$ is the volume fraction occupied by the particles, σ the effective particle diameter, and $a(q\sigma)$ the function defined by Hayter and Penfold.[25−27]

Results and Discussion

Micellar Structures at Low and High Concentrations. To analyze the ganglioside micellar surface charge, which depends on both temperature and the oligosaccharide chain, it is important to observe the effect of ganglioside concentration on scattering curves, namely, on micellar structures, since at a high concentration the scattering curves reflect not only a micellar structure but also an intermicellar interaction. Figure 1 shows the scattering curves of the G_{M1}, G_{D1a}, and G_{T1b} solutions of 0.5 and 5% w/v at 10 °C. The significant decrease of the scattering intensity below $q \approx 0.014$ Å^{-1} is caused by the presence of a beam stopper. Compared with the scattering curves at low and high concentrations in Figure 1, there are evident differences in the scattering profiles below $q \approx 0.045$ Å^{-1}. Every scattering curve at high concentration has a broad peak at $q \approx 0.028$ Å^{-1} for G_{M1}, $q \approx 0.027$ Å^{-1} for G_{D1a}, and $q \approx 0.030$ Å^{-1} for G_{T1b}. These broad peaks are attributable to the presence of repulsive intermicellar interaction resulting from an oligosaccharide chain with one or more sialic acid residues. The apparent average nearest-neighbor intermicellar distance can be estimated to be $d \approx 209-233$ Å by using the relation $d = 2\pi/q_{peak}$. The good agreement between the scattering curves at low and high concentrations above $q \approx 0.045$ Å^{-1} indicates that the ganglioside micellar structures hold in the concentration range from 0.5 to 5% w/v.[17] Every scattering curve has a rounded peak at about 0.09−0.1 Å^{-1} and an evident minimum at about 0.06−0.07 Å^{-1}. This suggests that every solution contains highly monodispersed globular particles, namely, the ganglioside

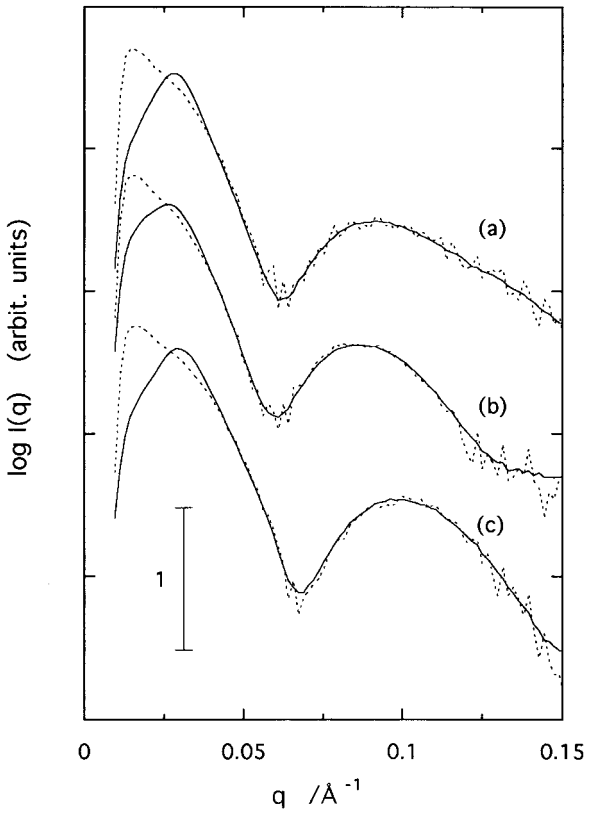

Figure 1. Scattering curves $I(q)$ of ganglioside solutions in pure water at 10 °C. Three different types of gangliosides were used: (a) G_{M1}, (b) G_{D1a}, and (c) G_{T1b}. Solid line and dotted line correspond to the ganglioside solutions with concentrations of 5% w/v and 0.5% w/v, respectively.

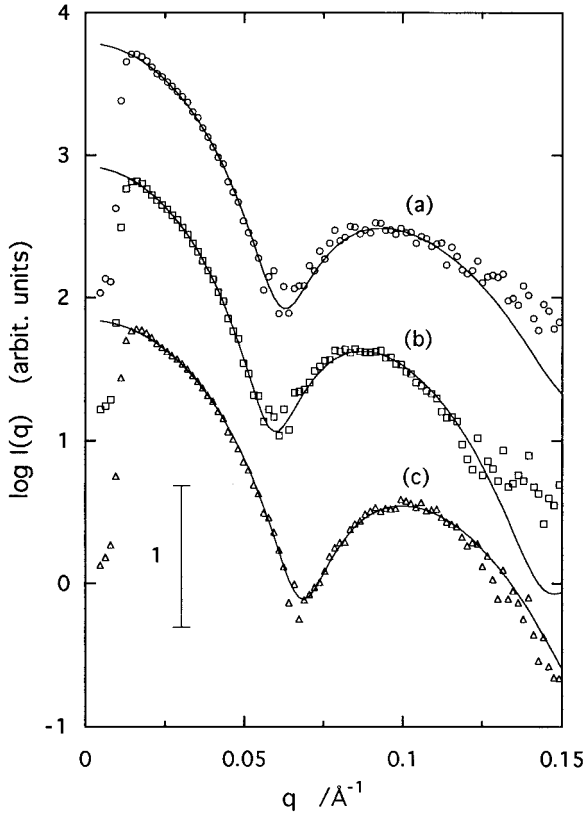

Figure 2. Double-shelled ellipsoid model fitting of the scattering curves of the 0.5% w/v ganglioside solutions in Figure 1. The scattering curves correspond to those of three different types of gangliosides, namely, (a) G_{M1}, (b) G_{D1a}, and (c) G_{T1b}. The symbols represent experimental data, and solid lines represent scattering curves obtained from double-shell ellipsoid models.

aggregates forming mostly identical micellar structures, and that the micelle holds the shape and the dimension in the concentration range we measured.

The difference in the scattering profiles of curves a−c of Figure 1 results from the difference in the ganglioside micellar structures that depend on the oligosaccharide chains. Clearly, the effect of the intermicellar interaction on the scattering curve at 0.5% w/v is negligibly small. As shown in Figure 2, we can fit very well the experimental scattering curves in Figure 1 with the model scattering functions using eq 4, where we simplified the ganglioside micellar structure as a double-shelled ellipsoid of rotation and used the scattering curves in the q range from 0.02 to 0.2 Å^{-1} for fitting. As in the previous results,[13,17] the agreement of the simulated scattering curve with the experimental one can be achieved only by using a double-shelled prolate ellipsoid, not by using a hard sphere or a hard ellipsoid. The reliability factors R for these models defined by

$$R = \sum \frac{|I_{obs}(q) - I_{model}(q)|}{\sum I_{obs}(q)}$$

are 0.047, 0.040, and 0.028, respectively. The determined structural parameters of the ganglioside micelles dispersed in pure water at 10 °C are as follows. For the G_{M1} micelle, the core and shell radii are 26.5 and 48.8 Å, the axial ratios are 1.67 and 1.55, and the ratio of the relative contrast values of the core and shell is −0.43/0.61. For the G_{D1a} micelle, the core and shell radii are 26.2 and 50.4 Å, the axial ratios are 1.36 and 1.46, and the ratio of the relative contrasts is −0.41/0.42. For the G_{T1b} micelle, the core and shell radii are 24.8 and 47.1 Å, the axial ratios are 1.36 and 1.41, and the ratio of the relative contrasts is −0.40/0.50. We can also estimate the gyration radius R_g by using eq 1. The R_g values obtained from the experimental scattering curves of the G_{M1}, G_{D1a}, and G_{T1b} solutions of 0.5% w/v at 10 °C are 52.5 ± 0.7 Å, 53.9 ± 0.6 Å, and 47.7 ± 0.6 Å, and the R_g values from the simulated scattering curves in Figure 2 are 52.9 ± 0.1 Å, 54.1 ± 0.1 Å, and 48.1 ± 0.1 Å, respectively. The experimental and simulated R_g values agree very well. The shell radius and the shell and core axial ratios obtained from the present experiments for the G_{M1} micelles are slightly larger than those shown in the previous results.[12] In the present experiments we dissolved gangliosides in pure water without buffer agents to minimize the electrostatic shielding effect by counterions. For this reason, the pH of the present solution becomes lower than that of the previous experiments of pH 6.8, which results in a slight expansion of the micellar structure as a general characteristic of ganglioside micelles on pH variation.[17] The difference in the structural parameters obtained from the present and previous results[13] is ascribed not only to the solvent conditions but also to the ganglioside species, since in the previous experiments we used a mixture of G_{D1a} and G_{D1b}. Despite such differences, the trends of the structural transitions responding to temperature and pH variations are common with each other as shown in the following section. By using the empirical expressions for a hydrocarbon chain volume[28] and the apparent atomic volumes of the basic chemical elements,[29] we can estimate tentatively the volumes of the hydrophilic head and hydrophobic tail of the ganglioside molecule. The volumes of the hydrophilic heads of the G_{M1}, G_{D1a}, and G_{T1b} molecules are 1215, 1525, and 1835 Å^3. The volume of the hydrophobic tail of the ceramide is 1029 Å^3. The average scattering densities of the head and tail portions are 1.23×10^{11} cm^{-2} for the G_{M1} head, 1.26×10^{11} cm^{-2} for the G_{D1a} head, 1.29×10^{11} cm^{-2} for the G_{T1b} head, and 8.69×10^{10} cm^{-2} for ceramide. Since the average scattering density of water is 9.4×10^{10} cm^{-2}, the values of contrast of the head and tail portions of the ganglioside molecule are 2.9×10^{10} cm^{-2} for the G_{M1} head, 3.2×10^{10} cm^{-2} for the G_{D1a} head, 3.5×10^{10} cm^{-2} for the G_{T1b} head, and -0.7×10^{10} cm^{-2} for ceramide. Then the apparent value of the ratio of the contrasts of the core and shell portions is given as −0.7/2.9 for G_{M1}, −0.7/3.2 for G_{D1a}, and −0.7/3.5 for G_{T1b}. The micellar hydrophobic core can be assumed to be virtually devoid of internal water, the same as in the cases of other hydrated phospholipid membranes.[30,31] In addition, the volume of the ceramide in the micelle can be assumed to be mostly constant in the temperature range measured, since hydrocarbon chains in the micelles contain many gauche configurations.[32−34] Then the ratio of the relative values of the contrasts of the shell and core portions obtained from the shell-modeling analysis is greatly different from the above empirical value of (2.9−3.5)/(−0.7), indicating the presence of a large amount of water in the hydrophilic shell region of the ganglioside micelle.[20] All structural parameters determined by the present shell-modeling methods are very reasonable to satisfy the physical constraints of micellar structures, which we previously showed in detail.[14−16,20]

Comparison and Analysis of Temperature Dependence of Changes of Micellar Structure, Surface Charge, and Intermicellar Interaction. Figure 3 shows the variation of the scattering curves of 5% w/v solutions for temperatures from 10 °C to 70 °C, where parts a, b, and c correspond to the G_{M1},

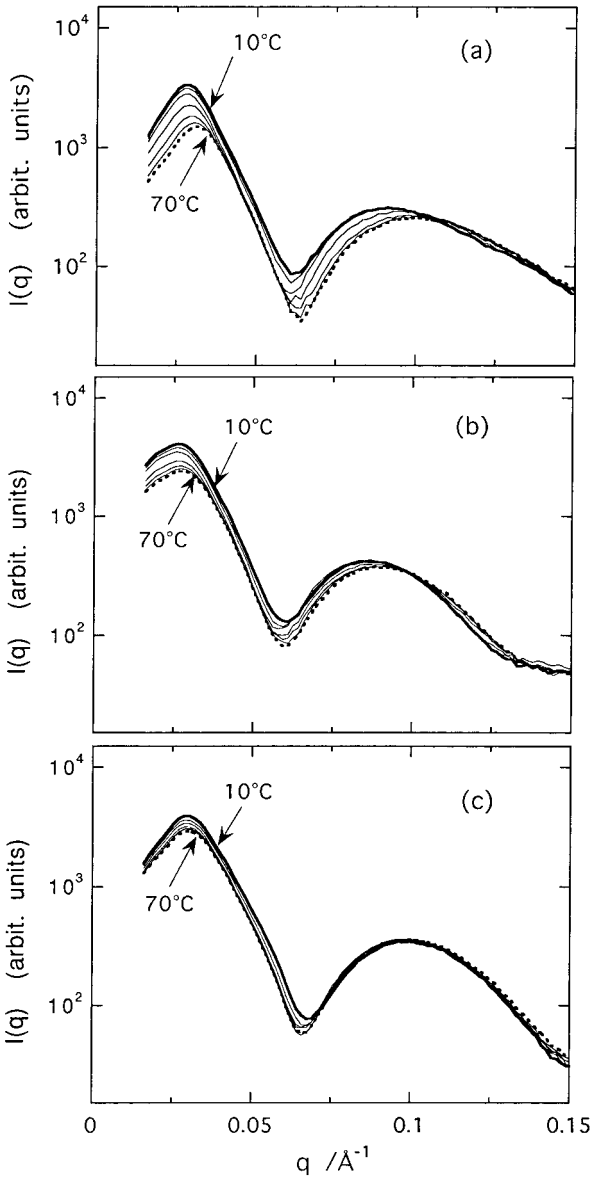

Figure 3. Temperature dependence of the scattering curves $I(q)$ of three different types of ganglioside solutions of 5% w/v in pure water: (a) G_{M1}; (b) G_{D1a}; (c) G_{T1b}. The temperature was elevated from 10 to 70 °C. Thick solid and dotted lines correspond to the scattering curves at 10 and 70 °C, respectively. The thin solid lines show the scattering curves at intermediate temperatures.

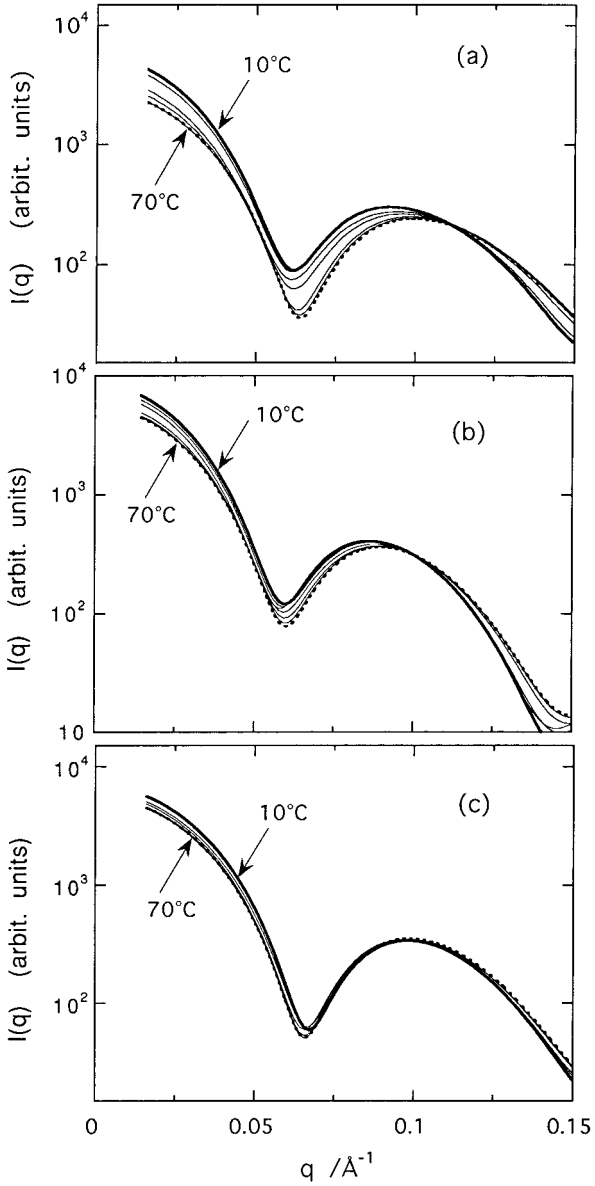

Figure 4. Simulated scattering curves $I_s(q)$ obtained by applying the double-shelled ellipsoid model fitting to the experimental scattering curves of the three different types of 5% w/v ganglioside solutions shown in Figure 3: (a) G_{M1}; (b) G_{D1a}; (c) G_{T1b}. For the model fitting, the experimental scattering data in the q range from 0.045 to 0.2 Å^{-1} were used.

G_{D1a}, and G_{T1b} solutions, respectively. As shown in the above section, the scattering curve above $q \approx 0.045$ Å^{-1} mostly depends on the ganglioside micellar structure, and the scattering curve below $q \approx 0.045$ Å^{-1} reflects the changes that occurred in both the micellar structure and the intermicellar interaction. We can recognize evident differences in the changing tendencies of the scattering curves of the G_{M1}, G_{D1a}, and G_{T1b} solutions in Figure 3; namely, the elevation of temperature induces a significant change of the scattering curve in the case of the G_{M1} solution and a minor change in the case of the G_{T1b} solution. The number of neutral sugars of each G_{M1}, G_{D1a}, and G_{T1b} ganglioside molecule is four. Therefore, the above evidence suggests that the effect of the temperature elevation on the ganglioside micellar structure greatly depends on the number of sialic acid residues in the oligosaccharide chain of the ganglioside molecule. With elevating temperature the G_{M1} solution shows the most significant changes of the position and height of the correlation peak at $q \approx 0.03$ Å^{-1}. This indicates that the micellar structural change accompanies a change of the interaction potential, which is discussed in detail in the following section.

As shown in Figure 1, the effect of the presence of intermicellar interaction on the scattering profile above $q \approx 0.045$ Å^{-1} is negligibly small even at a concentration of 5% w/v. Therefore, we used the shell-modeling method to fit the experimental scattering curves in the q range from 0.045 to 0.2 Å^{-1} and simulated the scattering curves $I_s(q)$ using eq 4. As shown in Figure 4, the simulated scattering curves $I_s(q)$ describe well the changes of the experimental scattering curves above 0.045 Å^{-1}. Despite the use of the experimental scattering data in the limited q range, the structural parameters obtained from the optimized double-shelled ellipsoid model of the 5% w/v ganglioside solutions at 10 °C mostly agree with those obtained from the 0.5% w/v ganglioside solutions at 10 °C within fitting error. For example, the determined structural parameters of the 5% w/v G_{M1} solution at 10 °C are the core and shell radii of

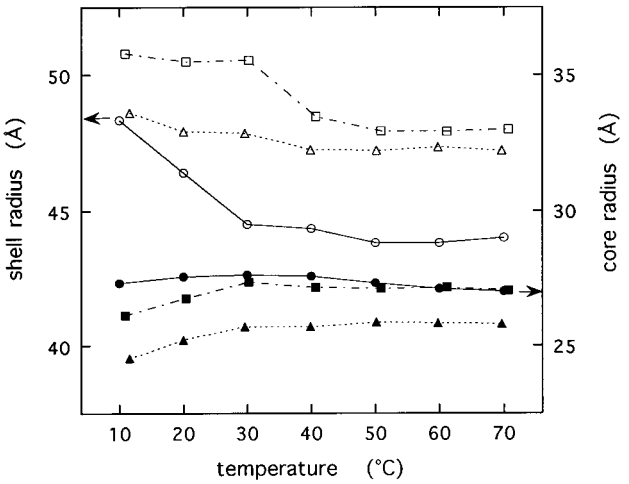

Figure 5. Temperature dependence of the shell and core radii of the three different types of ganglioside micelles determined from the scattering curves of the double-shelled ellipsoid models shown in Figure 3. Open and full symbols correspond to the shell and the core radii, respectively: (○, ●) G_{M1}; (□, ■) G_{D1}; (△, ▲) G_{T1b}.

27.3 and 48.3 Å, the axial ratios of 1.54 and 1.57, and the ratio of the relative contrast values of the core to the values of the shell of −0.43/0.59, where the reliability factor R is 0.072. These values mostly agree with the values obtained from the 0.5% w/v G_{M1} solution at 10 °C within fitting error. In Figure 5 we show the temperature dependence of structural parameters of the G_{M1}, G_{D1a}, and G_{T1b} micelles obtained from the shell-modeling analysis. The major change of the micellar structure is a decrease of the micellar hydrophilic region given by the difference between the shell and core radii. This changing aspect agrees with our previous results.[12−14] Although there are rather few data points on temperature, the midpoint of the main transition of the shrinkage of the micellar hydrophilic region can be assumed to be located at ∼20 °C for G_{M1}, ∼35 °C for G_{D1a}, and ∼25 °C for G_{T1b}. The above thermal transition features of the G_{M1} and G_{D1a} micelles in pure water, especially the shrinkage of the hydrophilic shell region, essentially agree with those of the previous results using buffer solvents around pH 7. The deviations of the transition temperature regions of the present experiments from those of the previous results are attributable to both the different solvent conditions and the different ganglioside species, as pointed out in the above section. Such a variation of the thermal transition feature subjected to the solvent condition would be general, as observed in other lipid micellar systems.[25]

Next, in Figure 6 we can deduce the intermicellar structure factor $S(q)$ in eq 3 by dividing the experimental scattering curve $I(q)$ in Figure 3 by the simulated scattering curve $I_s(q)$ in Figure 4. In the case of the G_{M1} solution in Figure 6a, the elevation of temperature induces an increase of the height of the correlation peak at $q \approx 0.031$ Å^{-1} in the temperature range from 10 to 30 °C with the peak position mostly constant and after that a gradual shift of the peak position from 0.031 to 0.036 Å^{-1} at 70 °C with decreasing peak height. Such a changing aspect is observed most evidently in Figure 6a of the G_{M1} solution. We can also recognize similar changing aspects in the G_{D1a} and G_{T1b} solutions in parts b and c of Figure 6; however, those aspects are minor compared with the G_{M1} case.

Under the scheme of the rescaled mean spherical approximation of interparticle interaction through a repulsive screened Coulomb potential,[25,26] the correlation peak profile of the interparticle structure factor $S(q)$ is known to depend on the effective diameter σ, the net charge z, and the number

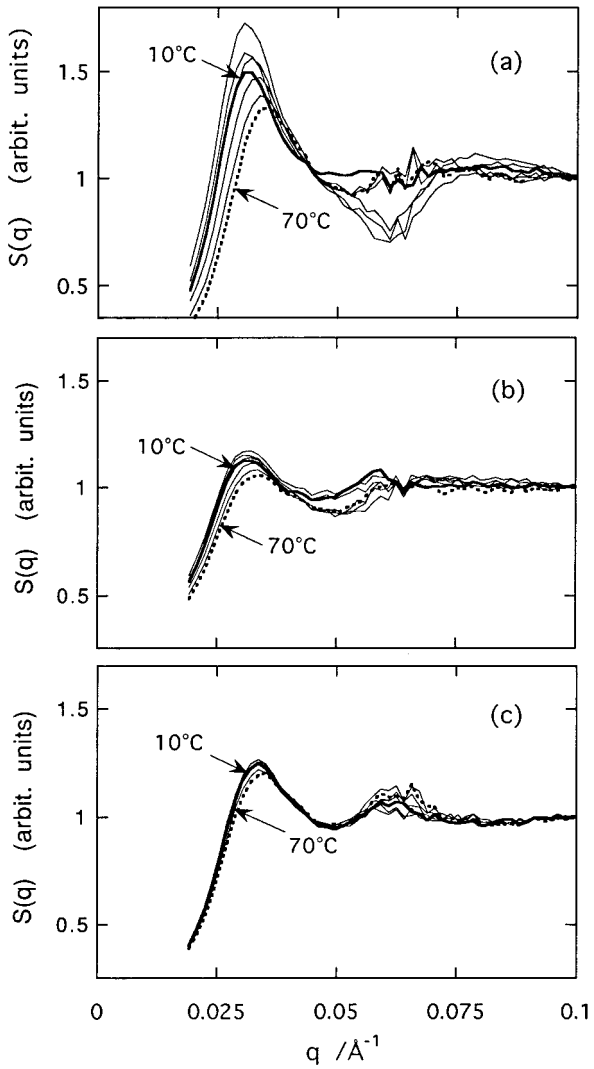

Figure 6. Intermicellar structure factors $S(q)$ obtained by dividing the experimental scattering curves in Figure 3 by the simulated scattering curves in Figure 4: (a) G_{M1}; (b) G_{D1a}; (c) G_{T1b}.

concentration N of the solute particle. In the case of ganglioside micelles the net charge z turns out to be the surface charge z of the micelle in the presence of sialic acid residues. According to the scheme reported previously,[17] we can estimate the z value as follows. Since we know the molar cencentration of ganglioside and the micellar shape and dimension obtained by the shell-modeling analysis, we can deduce the values of σ and N. Then we can use only the degree of ionization α of the micelle as a variable to fit the intermicellar structure factor $S(q)$ in Figure 7. The degree of the ionization α satisfies the relation of $z = \alpha n N_a$, where N_a is the average aggregation number of the micelle obtained by using the equation of N_a = (total volume of core)/(volume of ceramide) and n is the number of sialic acid residues of the ganglioside molecule. Thus, we can estimate the temperature dependence of the ionization degree α for G_{M1}, G_{D1a}, and G_{T1b} micelles, respectively. Here, we assumed that the critical micellar concentrations (cmc) of G_{M1}, G_{D1a}, and G_{T1b} micelles were 2.0×10^{-8}, 2.8×10^{-8}, and 3.9×10^{-8} M, respectively.[9] By using eq 6 based on the above scheme, we can obtain the best-fitted $S(q)$ functions of the ganglioside solution at different temperatures as shown in Figure 7, where we show the experimental and simulated $S(q)$ functions of the G_{M1} solution at three typical temperatures, namely, 10, 30, and 70 °C. The ionization degree α of the G_{M1} micelle increases once from 0.16 to 0.22 in the temperature range from 10 to 30

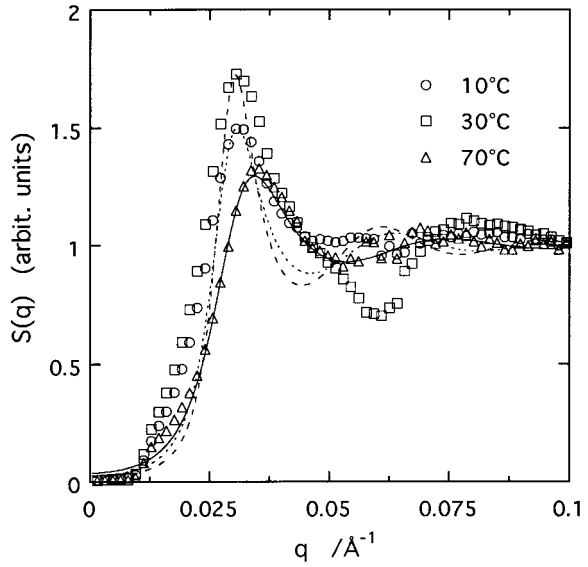

Figure 7. Simulated intermicellar structure factors $S(q)$ of the 5% w/v G_{M1} solution at three different temperatures, which were obtained by using eq 8 under the rescaled mean spherical approximation. ○, □, and △ marks correspond to the experimental $S(q)$ functions of 10, 30, and 70 °C in Figure 6a, respectively. The dotted, dashed, and solid lines show the simulated $S(q)$ functions of 10, 30, and 70 °C, respectively.

°C and after that decreases to 0.13 at 70 °C. Similar changing tendencies are obtained; that is, in the case of the G_{D1a} micelle, the α value increases from 0.25 to 0.3 in the range 10−20 °C and decreases to 0.2 at 70 °C, and in the case of the G_{T1b} micelle the α value increases from 0.4 to 0.5 in the range 10−30 °C and decreases to 0.3 at 70 °C.

Conclusion

In the present study, to analyze changes in both the structure and ionization degree of the micelle simultaneously from the experimental scattering curves, we have employed a procedure using a rescaled mean spherical approximation method (RMSA) for charged particle dispersions combined with a shell-modeling method, as used in a previous report.[17] This procedure can describe well the characteristics of the scattering curve showing an interparticle correlation peak for a micellar solution under a repulsive screened Coulomb potential. By using this procedure, we have found that the thermal structural change of the ganglioside micelle reported previously accompanies a change of the micellar surface charge, which greatly depends on the oligosaccharide chains. Namely, with elevating temperature the ionization degree α of the micelle slightly increases once, and afterward, it decreases evidently around the structural transition temperature. Such changes in the structure and ionization degree of the micelle occur most significantly for the G_{M1} case, moderately for the G_{D1a} case, and weakly for the G_{T1b} case. In the previous studies we reported that in the thermal structural change of ganglioside micelles the shrinkage of the hydrophilic region and the slight expansion of the hydrophobic region of the micelle occur in the physiological temperature range 20−40 °C.[12,13] Recently, we executed additional analyses of those results and showed clear evidence of reversible extrusion and occlusion of a large amount of water in the hydrophilic region of the ganglioside micelle in the temperature range 6−60 °C.[15] In this report we discussed that the estimated number of water molecules in the hydrophilic shell region of the ganglioside micelle includes not only hydrated water but also a large amount of nearly free water.

Combined with the those previous results, we consider as follows. With elevating temperature two different events compete with each other. One is the increase of the dissociation degree of sialic acids as a general trend of acidic residues, and the other is the shrinkage of the oligosaccharide chain conformations. At relatively low temperatures such as ca. 10−30 °C, the former event occurs first before the latter event and strengthens repulsive intermicellar interactions. After that, at high temperatures above ca. 40 °C the latter event reduces the penetration of water into the hydrophilic oligosaccharide chain region, which results in the decrease of the dissociation degree of sialic acid residues. The monotonic trend for water extrusion in the case of the G_{M1} micelle at low temperature[15] would mainly reflect the extrusion of nearly free water. This reasonably explains the present findings, that is, an initial increase of the dissociation degree of sialic acids and then a decease for the higher temperatures.

Gangliosides are known to participate in various important cell surface events such as a molecular recognition and cell differentiation through a variety of oligosaccharide chains. In addtion, recent studies show that gangliosides are organized to form microdomains called "raft" structures in outer cell membranes, which are assumed to be essentially important for gangliosides as inducers of signal transduction.[36,37] Therefore, the intrinsic properties of the ganglioside aggregates found in our present and previous studies strongly suggest that ganglioside microdomains in an outer cell membrane are able to modulate both charge and hydrophilicity of the cell surface. Such abilities of gangliosides for various external conditions greatly depend on the variety of oligosaccharide chains, which would result in a direct or indirect regulation of various cell surface events such as adhesion between cells or protein binding to the cell surface.

Acknowledgment. This work was done under the approval of the Photon Factory Programme Advisory Committee (Proposal No. 95G084 & 98G185).

References and Notes

(1) Makita, A.; Taniguchi, N. In *Glycosphingolipid*; Weigandt, H., Ed.; Elsevier: New York, 1985, 59.
(2) Hansson, H. A.; Holmgren, J.; Svennerholm, L. *Proc. Natl. Acad. Sci. U.S.A.* **1977**, *74*, 141.
(3) Hannun, Y. A.; Bell, R. M. *Science* **1989**, *243*, 500.
(4) Hakomori, S.; Igarashi, Y. *Adv. Lipid Res.* **1993**, *25*, 147.
(5) Svennerholm, L.; Asbury, A. K.; Reisfeld, R. A.; Sandhoff, K.; Suzuki, K.; Tettamanti, G.; Toffano, G. Biological Function of Gangliosides; Elsevier: Amsterdam, 1994.
(6) Tettamanti, G.; Sonnion, S.; Ghidoni, R.; Masserini, M.; Venerando, B. In *Physics of Amphiphiles: Micelles, Vesicles and Microemulsions*; Corti, M., Degiorgio, V., Eds.; North-Holland: Amsterdam, 1985; p 607.
(7) Maggio, B.; Ariga, T.; Sturtevant, J. M.; Yu, R. K. *Biochim. Biophys. Acta* **1985**, *818*, 1.
(8) Corti, M.; Cantù, L. *Adv. Colloid Interface Sci.* **1990**, *32*, 151.
(9) Sonnion, S.; Cantù, L.; Corti, M.; Acquotti, D.; Venerando, B. *Chem. Phys. Lipids* **1994**, *71*, 21.
(10) van Gorkom, L. C. M.; Cheetham, J. J.; Epand, R. M. *Chem. Phys. Lipids* **1995**, *76*, 103.
(11) Hirai, M.; Yabuki, S.; Takizawa, T.; Nakata, Y.; Mitomo, H.; Hirai, T.; Shimizu, S.; Kobayashi, K.; Furusaka, M.; Hayashi, K. *Physica B* **1995**, *213&214*, 748.
(12) Hirai, M.; Takizawa, T.; Yabuki, S.; Nakata, Y.; Hayashi, K. *Biophys. J.* **1996**, *70*, 1761.
(13) Hirai, M.; Takizawa, T.; Yabuki, S.; Hirai, T.; Hayashi, K. *J. Phys. Chem.* **1996**, *100*, 11675.
(14) Hirai, M.; Arai, S.; Takizawa, T.; Yabuki, S.; Nakata, Y. *Thermochim. Acta* **1998**, *308*, 93.
(15) Hirai, M.; Takizawa, T. *Biophys. J.* **1998**, *74*, 3010.
(16) Hirai, M.; Takizawa, T. *J. Phys. Chem. B* **1998**, *102*, 3062.
(17) Hirai, M.; Takizawa, T.; Yabuki, S.; Hayashi, K. *J. Chem. Soc., Faraday Trans.* **1996**, *92*, 4533.

(18) Hirai, M.; Takizawa, T.; Yabuki, S.; Nakata, Y.; Mitomo, H.; Hirai, T.; Shimizu, S.; Furusaka, M.; Kobayashi, K.; Hayashi, K. *Physica B* **1995**, *213&214*, 751.

(19) Takizawa, T.; Hirai, M.; Yabuki, S.; Nakata, Y.; Takahashi, A.; Hayashi, K. *Thermochim. Acta* **1995**, *267*, 355.

(20) Hirai, M.; Iwase, H.; Arai, S.; Takizawa, T.; Hayashi, K. *Biophys. J.* **1998**, *74*, 1380.

(21) Ueki, T.; Hiragi, Y.; Kataoka, M.; Inoko, Y.; Amemiya, Y.; Izumi, Y.; Tagawa, H.; Muroga, Y. *Biophys. Chem.* **1985**, *23*, 115.

(22) Glatter, O. In *Small Angle X-ray Scattering*; Glatter, O., Kratky, O., Eds.; Academic Press: London, 1982; p 119.

(23) Hirai, M.; Takizawa, T.; Yabuki, S.; Kawai-Hirai, R.; Nakamura, K.; Kobayashi, K.; Amemiya, Y.; Oya, M. *J. Chem. Soc., Faraday Trans.* **1995**, *91*, 1081.

(24) Hirai, M.; Kawai-Hirai, R.; Takizawa, T.; Yabuki, S.; Hirai, T.; Kobayashi, K.; Amemiya, Y.; Oya, M. *J. Phys. Chem.* **1995**, *99*, 6652.

(25) Hayter, J. B.; Penfold, J. *Mol. Phys.* **1981**, *42*, 109.

(26) Hayter, J. B.; Penfold, J. *J. Chem. Soc., Faraday Trans. 1* **1981**, *77*, 1851.

(27) Hansen, J. P.; Hayter, J. B. *Mol. Phys.* **1982**, *46*, 651.

(28) Israelachvili, J. N.; Mitchell, D. J.; Ninham, B. W. *J. Chem. Soc., Faraday Trans. 2II.* **1976**, *72*, 1525.

(29) Zamyatin, A. A. *Prog. Biophys. Mol. Biol.* **1972**, *24*, 107.

(30) Worcester, D. L.; Franks, N. P. *J. Mol. Biol.* **1976**, *100*, 359.

(31) Büldt, G.; Gally, H. U.; Seelig, A.; Seelig, J.; Zaccai, G. *Nature* **1978**, *217*, 182.

(32) Dill, K. A.; Koppel, D. E.; Cantor, R. S.; Dill, J. D.; Bendedouch, D.; Chen, S.-H. *Nature* **1984**, *309*, 42.

(33) Gruen, D. W. R. *J. Colloid Interface Sci.* **1981**, *84*, 281.

(34) Gruen, D. W. R.; de Lacey, E. H. B. In *Surfactants in Solution*; Mittel, K. L., Lindman, B., Eds.; Plenum Press: New York, 1984; Vol. 1, p 279.

(35) Hirai, M.; Takizawa, T.; Yabuki, S.; Hirai, T.; Hayashi, K. *J. Phys. Chem.* **1995**, *99*, 17456.

(36) Simons, K.; Ikonen, E. *Nature* **1997**, *387*, 569.

(37) Hakomori, S.; Yamamura, S.; Handa, K. In *Sphingolipids as signaling modulators in the nervous system*; Ledeen, R. W., Hakomori, S., Yates, A., Scheider, J. S., Yu, R. K., Eds.; The New York Academy of Sciences: New York, 1998, p 1.